

Published in final edited form as:

Science. 2014 February 28; 343(6174): 1010–1014. doi:10.1126/science.1249484.

Detection of a Recurrent *DNAJB1-PRKACA* Chimeric Transcript in Fibrolamellar Hepatocellular Carcinoma

Joshua N. Honeyman^{1,2,*}, Elana P. Simon^{1,3,*}, Nicolas Robine^{4,*}, Rachel Chiaroni-Clarke¹, David G. Darcy^{1,2}, Irene Isabel P. Lim^{1,2}, Caroline E. Gleason¹, Jennifer Murphy^{1,2}, Brad R. Rosenberg⁵, Lydia Teegan¹, Constantin N. Takacs¹, Sergio Botero¹, Rachel Belote¹, Soren Germer⁴, Anne-Katrin Emde⁴, Vladimir Vacic⁴, Umesh Bhanot⁶, Michael P. LaQuaglia², and Sanford M. Simon^{1,†}

¹Lab of Cellular Biophysics, Rockefeller University, 1230 York Avenue, New York, NY 10065

²Division of Pediatric Surgery, Department of Surgery; Memorial Sloan-Kettering Cancer Center; 1275 York Avenue; New York, NY 10065.

³The Dalton School, 108 East 89th Street, New York, NY 10128

⁴New York Genome Center, 101 Avenue of the Americas, New York, NY 10013

⁵Whitehead Presidential Fellows Program, The Rockefeller University, 1230 York Avenue, New York, NY 10065

⁶Pathology Core Facility Memorial Sloan-Kettering Cancer Center; 1275 York Avenue; New York, NY 10065

Abstract

Fibrolamellar hepatocellular carcinoma (FL-HCC) is a rare liver tumor affecting adolescents and young adults who have no history of primary liver disease or cirrhosis. We performed RNA sequencing on FL-HCC tumors and identified a chimeric transcript that was expressed in all tumor samples but not in adjacent normal liver. The chimeric RNA was confirmed by RT-PCR and Sanger Sequencing. Based on the results of whole genome sequencing, the chimeric transcript is the result of a ~400 kilobase deletion on chromosome 19. The chimera was predicted to code for a protein with the amino-terminal domain of DNAJB1, a homolog of the molecular chaperone DNAJ, fused in frame with PRKACA, the catalytic domain of protein kinase A. The presence of this chimera protein was established by immunoprecipitation and Western Blot analysis. Expression of the chimera in human cell culture demonstrates that it retains kinase activity. Evidence for a DNAJB1-PRKACA chimeric transcript in 15 out of 15 FL-HCC patients suggests that it contributes to tumor pathogenesis.

Main Text

Fibrolamellar hepatocellular carcinoma (FL-HCC) is a rare liver tumor representing less than 1% of all liver cancer(1). First described in 1956(2), it has historically been considered

[†]Corresponding author. simon@rockefeller.edu.
^{*}co first authors

a variant of hepatocellular carcinoma. It is histologically characterized by well-differentiated neoplastic hepatocytes and thick fibrous bands in a non-cirrhotic background(3, 4). FL-HCC has a distinct clinical phenotype in comparison to conventional hepatocellular carcinoma and usually occurs in adolescents and young adults. Patients have normal levels of alpha fetoprotein without underlying liver disease or history of viral hepatitis (3–6). Little is known of its molecular pathogenesis. FL-HCC tumors do not respond well to chemotherapy(7, 8) and surgical resection remains the mainstay of therapy with overall survival reported to be 30 to 45% at five years(1, 6, 8, 9).

To investigate the molecular basis of FL-HCC, we performed whole transcriptome and whole genome sequencing of paired tumor and adjacent normal liver samples. To identify if there were possible fusion transcripts among the coding RNA, we ran the program FusionCatcher (10) on RNA-seq data from 29 samples, including primary tumors, metastases, recurrences and matched normals, derived from a total of 11 patients (Supplementary Table 1). This analysis identified variable candidate fusions (range 3 to 16) for each tumor sample. There was only one recurrent candidate chimeric transcript detected in every tumor sample. This candidate transcript is predicted to result from the in-frame fusion of exon 1 from *DNAJB1*, a member of the heat shock 40 protein family, with exons 2–10 from *PRKACA* which encodes the cAMP-dependent protein kinase A (PKA) catalytic subunit alpha. This fusion transcript was not detected in any of the available paired normal tissue samples (n=9). This fusion is not found in the Cosmic database (11), and has not previously been reported in the literature.

To further characterize the candidate fusion transcript, we directly examined those RNA-Seq reads that mapped to *PRKACA* and *DNAJB1*. We examined *PRKACA* transcript levels with DESeq2 (12), and found they were increased compared to normal in all 9 patients tested ($p_{\text{Adj}} < 10^{-12}$, range 3 to 8 fold). To test if the increased expression was attributable to a specific isoform of *PRKACA*, we quantified reads mapping to different exons and evaluated differential expression using DEXSeq (13). In all nine patients, there was an increase in the expression of exons 2–10 of *PRKACA* in the tumor relative to exon 1 and relative to the expression in normal tissue (Fig 1A, left). This exon expression pattern does not correspond to a known isoform of *PRKACA*. Rather, it reflects an increase in *PRKACA* transcripts which lack the first exon, which encodes the domain that engages the regulatory subunits of PKA. All reads mapping to *PRKACA* in normal tissue were either contained within exons or bridged the junctions between adjacent exons at annotated splicing sites (Fig 1B, left, blue). All tumor samples additionally had reads mapping from the start of the second exon of *PRKACA* to a point ~400 kilobases (kb) upstream relative to the coding, corresponding to the end of the first exon of *DNAJB1* (marked with an * Fig. 1B, red). Examination of the exon expression of *DNAJB1* in tumor samples revealed a decrease in the number of reads in exons 2 and 3 relative to exon 1 (Fig 1A, B, right). The data on the differential exon expression and the data on the RNA-seq reads spanning the 400kb distance that bridges these two genes, further support a structural variation resulting in a chimeric transcript incorporating *DNAJB1* and *PRKACA*.

In tumor samples from patients 4 and 14, there were indications of a second splice variant spanning *PRKACA* and *DNAJB1* (Fig 1C). In addition to the reads from the end of exon 1

of DNAJB1 to the start of exon 2 of PRKACA (Fig 1C middle red plot marked with a * and Fig 1D, the predominant chimera), there were reads that started in the middle of exon 2 of DNAJB1 and mapped to the start of exon 2 of PRKACA (Fig 1C middle red plot marked with a ** and Fig 1D, the minority chimera). For patient 4 we also sequenced four different metastases and observed reads that spanned the same regions (Fig 1C bottom red plot). These findings predict the presence of one predominant chimera incorporating only the first exon of DNAJB1, and a second, minority chimera incorporating both the first and a portion of the second exon of DNAJB1. Both chimeras continue with exons 2–10 of PRKACA.

The presence of the predicted dominant chimeric RNA transcript was validated by Sanger sequencing of reverse transcription polymerase chain reaction (RT-PCR) products in all 7 tumor samples tested from 6 patients (Fig 1E), including one tumor/recurrence pair. The same chimeric transcript was confirmed by Sanger sequencing in an eighth newly acquired primary tumor from a patient whose samples were not previously analyzed by RNA-seq or whole genome sequencing.

In every tumor sample, in addition to the presence of one or both predicted RNA chimeras, we also observed RNA-Seq reads consistent with transcripts covering the entire length of PRKACA, suggesting the cells still contain a wild type copy of the gene. These results are most consistent with a heterozygous deletion in chromosome 19 resulting in a single copy of the chimeric transcript and single copies of both the WT DNAJB1 and the WT PRKACA.

We next searched for potential structural variants in the FL-HCC genome by performing whole-genome sequencing on paired tumor and adjacent normal liver. We used the program Delly (11) to search for structural variations on chromosome 19. In eight of ten tumor samples, there were between 2 and 23 paired-end reads that spanned ~400 kb and mapped to both DNAJB1 and PRKACA. In addition, in all eight of these tumor samples, split-reads mapped to the deletion fusion point (Supplemental Table 2). The program, SplazerS (14) identified 3–17 split-reads mapping between these genes in all ten tumor samples. The predicted deletions ranged in size from 401,552 to 409,262 base pairs (bp), with a telomeric breakpoint between chr19: 14,218,306-14,226,300 (hg19) and a centromeric breakpoint between chr19: 14,627,567-14,628,632. These deletions were not detected in adjacent normal liver samples.

The presence of the predicted deletion in the tumor DNA was validated by PCR and Sanger sequencing in eight out of eight samples tested (Fig 2B). In all patients, the precise breakpoints of the deletion mapped to different genomic coordinates (Supplemental Table 2). For all patients, the data were consistent with a deletion originating in the first intron (n= 6) or the second exon (n= 4) of DNAJB1 and terminating in the first intron of PRKACA (Fig 2A).

To determine whether the chimeric RNA transcript was translated into a chimeric protein, we performed Western Blot analysis. Proteins extracted from tumor and adjacent normal liver samples were separated by SDS-PAGE, and probed with an antibody to the carboxyl terminus of PRKACA. Normal and tumor samples showed a band corresponding to a size of 41 kDa (Fig 3A), the predicted size of isoform 1 of wild-type (WT) PRKACA. In nine of

nine previously sequenced tumor samples, there was a slower moving band at ~46 kDa consistent with the predicted larger molecular size of the predominant chimeric protein (patients 1, 3, 4, 5, 6, 7, 10, 11, 12). This higher molecular weight band was not observed in any of the normal samples. Additional pairs of tumor and normal tissue not originally sequenced (patients 13, 14, 17) were analyzed and showed the same larger band in the tumor but not in the normal. The larger band was also seen in two metastases from patient 2.

We observed a third immunoreactive band in samples from two patients that migrated at ~50 kD (Fig 3A patients 4 and 14), consistent with the minority chimera predicted by the RNA-seq analysis. This larger band was present in addition to the bands corresponding to the native PRKACA and the predominant DNAJB1-PRKACA chimera. This slower mobility, apparently higher molecular weight band is consistent with a chimera that includes the first exon and portion of exon 2 of DNAJB1, as well as exons 2–10 of PRKACA (Fig 1C, patient 4 shown).

To confirm that the higher bands were the chimeric proteins we tested if they were recognized by antibodies to both the amino-terminus of DNAJB1 and the carboxyl-terminus of PRKACA. Protein was immunoprecipitated with an antibody to DNAJB1, separated by SDS-PAGE alongside a sample of the total solubilized tissue, and then probed on a Western Blot with an antibody to the carboxyl-terminus of PRKACA (Fig 3B). The whole cell lysate again showed bands at the corresponding to both the WT PRKACA and the chimera. However, the sample immunoprecipitated with DNAJB1 showed only the higher molecular weight band (lanes labeled IP-DNAJB1, fig 3B) corresponding to the chimera. The WT PRKACA band was not present in the immunoprecipitate. Thus, the higher molecular weight band that is present only in tumor samples is a true chimeric protein resulting from the fusion of the amino-terminus of DNAJB1 and carboxyl-terminus of PRKACA.

To determine whether the DNAJB1-PRKACA chimeric protein retains kinase activity, we transfected HEK-293T (human embryonic kidney) cells with plasmids encoding either WT PRKACA or the DNAJB1-PRKACA chimera. Control cells were transfected with an “empty” plasmid lacking the PRKACA or chimera genes, thereby providing a measure for the background activity level of PKA in the cells. PKA activity was measured by the ability of cell lysate to phosphorylate the fluorescent PKA substrate peptide LRRASLG whose mobility shifts on a gel upon phosphorylation. In cells expressing either WT PRKACA or the chimera (Fig 3D), PKA activity was significantly greater than controls ($p < 0.001$, Fig 3D). Both PRKACA and the chimera were each expressed from the same promoter, and the PKA activity was indistinguishable in cells expressing either protein. This demonstrates that the chimeric protein retains full PKA activity.

Using confocal fluorescence microscopy we examined the expression of PRKACA in tumor and adjacent normal tissue. Using an antibody against the carboxyl-terminus of PRKACA, the resulting fluorescent signal was consistently brighter throughout the cells in FL-HCC (Fig 3E and supplemental Fig 1) compared to the adjacent tissue normal liver (Fig 3D).

In summary, we have provided evidence for a 400 kb heterozygous deletion on chromosome 19 in ten out of ten FL-HCC patients tested. We detected a chimeric DNAJB1- PRKACA

RNA transcript in 12 of 12 patients tested and we detected a putative chimeric DNAJB1-PRKACA protein in 14 of 14 patients tested. Neither the genomic deletion, the chimeric transcript, nor the chimera protein were present in any normal liver samples tested. This chimera is predicted to incorporate the J domain of DNAJB1 and the catalytic domain of PRKACA. The promoter is from the DNAJB1 gene, which could explain the higher transcription of the chimera compared to the WT PRKACA (Fig 1A, B, C).

PKA is a heterotetramer composed of two regulatory subunits and two catalytic subunits. In this configuration, the catalytic subunit is inactive until cAMP binding causes its release from the regulatory units. The DNAJB1-PRKACA chimera retains the functional catalytic domain and maintains full kinase activity, but it is missing the domain that binds the regulatory subunits of PKA. PKA phosphorylates numerous cytoplasmic and nuclear substrates, including members of the Ras, MAPK (15), estrogen signaling(16), and apoptosis pathways(17). PKA is also involved in signaling via EGFR(18) and regulation of aromatase expression(19), both of which can be overexpressed in FL-HCC(20–23). PRKACA has been implicated in epithelial-mesenchymal transition, migration and invasion in lung cancer cells(24). A review of publically available data sets from The Cancer Genome Atlas (25, 26) suggests that PRKACA is amplified in 12% of ovarian serous cystadenocarcinoma(27), 5% of uterine corpus endometrial carcinoma(28), 3% of adenoid cystic carcinoma(29), 2% of lung squamous cell carcinoma(30), 1% of sarcoma(31), colon and rectum adenocarcinoma(32) and breast invasive carcinoma(33). In FL-HCC, the deletion we observe in chromosome 19 has not been reported in comparative genomic hybridization of FL-HCC (34–37), perhaps due to the limited resolution of the approach at the time those studies were performed.

There are currently no molecular diagnostic tests for FL-HCC. Since previous studies have detected PKA in the peripheral blood of cancer patients (38), this chimera may represent a diagnostic marker for FL-HCC. Surgical resection remains the cornerstone of therapy and patients who present with advanced stage or metastatic disease have few treatment options. While the role of the DNAJB1-PRKACA chimera in the pathogenesis of FL-HCC has yet to be addressed, our observations raise the possibility that it contributes to the pathogenesis of the tumor and may represent a therapeutic target.

Supplementary Material

Refer to Web version on PubMed Central for supplementary material.

Acknowledgment

This work was supported by a grant from The Fibrolamellar Cancer Foundation, RUCCTS Grant #2UL1RR024143, and Friends of Gerry and Diane Smallberg, Matthew Lynch and Josh Panda. Constantin Takacs was supported by a Howard Hughes Medical Institute International Student Predoctoral Fellowship. We are grateful to our colleagues Sohail Tavazoie, Hani Goodarzi, and Bob Darnell for their support, insightful discussions of the data and critical comments on the manuscript. Thanks to the Pathology core facility (MSKCC), the Molecular Cytology core facility (MSKCC) and members of the Fibrolamellar community, including Marna Davis, Gail Trecosta, and Rachael Migler for support.

References

1. El-Serag HB, Davila JA. Is fibrolamellar carcinoma different from hepatocellular carcinoma? A US population-based study. 2004; 39:798–803.
2. Edmondson HA. Differential diagnosis of tumors and tumor-like lesions of liver in infancy and childhood. 1956; 91:168–186.
3. Torbenson M. Review of the clinicopathologic features of fibrolamellar carcinoma. 2007; 14:217–223.
4. Craig JR, Peters RL, Edmondson HA, Omata M. Fibrolamellar carcinoma of the liver: a tumor of adolescents and young adults with distinctive clinico-pathologic features. 1980; 46:372–379.
5. Stipa F, et al. Outcome of patients with fibrolamellar hepatocellular carcinoma. 2006; 106:1331–1338.
6. Mavros MN, Mayo SC, Hyder O, Pawlik TM. A Systematic Review: Treatment and Prognosis of Patients with Fibrolamellar Hepatocellular Carcinoma. 2012
7. Weeda VB, et al. Fibrolamellar variant of hepatocellular carcinoma does not have a better survival than conventional hepatocellular carcinoma - Results and treatment recommendations from the Childhood Liver Tumour Strategy Group (SIOPEL) experience. 2013
8. Katzenstein HM, et al. Fibrolamellar hepatocellular carcinoma in children and adolescents. 2003; 97:2006–2012.
9. Kakar S, et al. Clinicopathologic features and survival in fibrolamellar carcinoma: comparison with conventional hepatocellular carcinoma with and without cirrhosis. 2005; 18:1417–1423.
10. Edgren H, et al. Identification of fusion genes in breast cancer by paired-end RNA-sequencing. *Genome Bio.* 2011; 12:R6. [PubMed: 21247443]
11. Bamford S, et al. The COSMIC (Catalogue of Somatic Mutations in Cancer) database and website. *Br. J. Cancer.* 2004; 91:355–358. [PubMed: 15188009]
12. Anders S, Huber W. Differential expression analysis for sequence count data. *Genome Biol.* 2010; 11:R106. [PubMed: 20979621]
13. Reyes A, Anders S, Huber W. Analyzing RNA-seq data for differential exon usage with the DEXSeq package. 2012
14. Emde A-K, et al. Detecting genomic indel variants with exact breakpoints in single- and paired-end sequencing data using SplazerS. *Bioinformatics.* 2012; 28:619–627. [PubMed: 22238266]
15. Adams DG, Sachs NA, Vaillancourt RR. Phosphorylation of the stress-activated protein kinase, MEKK3, at serine 166. *Archives of biochemistry and biophysics.* 2002; 407:103–116. [PubMed: 12392720]
16. Chen D, Pace PE, Coombes RC, Ali S. Phosphorylation of human estrogen receptor alpha by protein kinase A regulates dimerization. *Molecular and cellular biology.* 1999; 19:1002–1015. [PubMed: 9891036]
17. Datta SR, et al. 14-3-3 proteins and survival kinases cooperate to inactivate BAD by BH3 domain phosphorylation. *Molecular cell.* 2000; 6:41–51. [PubMed: 10949026]
18. Tortora G, et al. The R1alpha subunit of protein kinase A (PKA) binds to Grb2 and allows PKA interaction with the activated EGF-receptor. *Oncogene.* 1997; 14:923–928. [PubMed: 9050991]
19. Bouchard MF, Taniguchi H, Viger RS. Protein kinase A-dependent synergism between GATA factors and the nuclear receptor, liver receptor homolog-1, regulates human aromatase (CYP19) PII promoter activity in breast cancer cells. 2005; 146:4905–4916.
20. Muramori K, et al. High aromatase activity and overexpression of epidermal growth factor receptor in fibrolamellar hepatocellular carcinoma in a child. *Journal of pediatric hematology/oncology.* 2011; 33:e195–e197. [PubMed: 21552145]
21. Patonai A, et al. Molecular Characteristics of Fibrolamellar Hepatocellular Carcinoma. *Pathology oncology research : POR.* 2012
22. Ang CS, et al. Clinicopathologic characteristics and survival outcomes of patients with fibrolamellar carcinoma: data from the fibrolamellar carcinoma consortium. *Gastrointestinal cancer research : GCR.* 2013; 6:3–9. [PubMed: 23505572]

23. Buckley AF, Burgart LJ, Kakar S. Epidermal growth factor receptor expression and gene copy number in fibrolamellar hepatocellular carcinoma. *Human pathology*. 2006; 37:410–414. [PubMed: 16564914]
24. Shaikh D, et al. cAMP-dependent protein kinase is essential for hypoxia-mediated epithelial-mesenchymal transition, migration, and invasion in lung cancer cells. *Cellular signalling*. 2012; 24:2396–2406. [PubMed: 22954688]
25. Cerami E, et al. The cBio cancer genomics portal: an open platform for exploring multidimensional cancer genomics data. *Cancer discovery*. 2012; 2:401–404. [PubMed: 22588877]
26. Gao J, et al. Integrative analysis of complex cancer genomics and clinical profiles using the cBioPortal. *Science signaling*. 2013; 6:p11. [PubMed: 23550210]
27. Cancer Genome Atlas Research Network. Integrated genomic analyses of ovarian carcinoma. *Nature*. 2011; 474:609–615. [PubMed: 21720365]
28. Cancer Genome Atlas Research Network. Integrated genomic characterization of endometrial carcinoma. *Nature*. 2013; 497:67–73. [PubMed: 23636398]
29. Ho AS, et al. The mutational landscape of adenoid cystic carcinoma. *Nat. Genet*. 2013; 45:791–798. [PubMed: 23685749]
30. Cancer Genome Atlas Research Network. Comprehensive genomic characterization of squamous cell lung cancers. *Nature*. 2012; 489:519–525. [PubMed: 22960745]
31. Barretina J, et al. Subtype-specific genomic alterations define new targets for soft-tissue sarcoma therapy. *Nat. Genet*. 2010; 42:715–721. [PubMed: 20601955]
32. Cancer Genome Atlas Network. Comprehensive molecular characterization of human colon and rectal cancer. *Nature*. 2012; 487:330–337. [PubMed: 22810696]
33. Cancer Genome Atlas Network. Comprehensive molecular portraits of human breast tumours. *Nature*. 2012; 490:61–70. [PubMed: 23000897]
34. Wilkens L, et al. Cytogenetic aberrations in primary and recurrent fibrolamellar hepatocellular carcinoma detected by comparative genomic hybridization. 2000; 114:867–874.
35. Kakar S, et al. Chromosomal changes in fibrolamellar hepatocellular carcinoma detected by array comparative genomic hybridization. 2009; 22:134–141.
36. Ward SC, Waxman S. Fibrolamellar carcinoma: a review with focus on genetics and comparison to other malignant primary liver tumors. 2011; 31:61–70.
37. Marchio A, et al. Distinct chromosomal abnormality pattern in primary liver cancer of non-B. non-C patients. 2000; 19:3733–3738.
38. Nesterova MV, et al. Autoantibody cancer biomarker: extracellular protein kinase A. *Cancer Res*. 2006; 66:8971–8974. [PubMed: 16982736]
39. Katz Y, Wang ET, Airolidi EM, Burge CB. Analysis and design of RNA sequencing experiments for identifying isoform regulation. *Nat. Methods*. 2010; 7:1009–1015. [PubMed: 21057496]

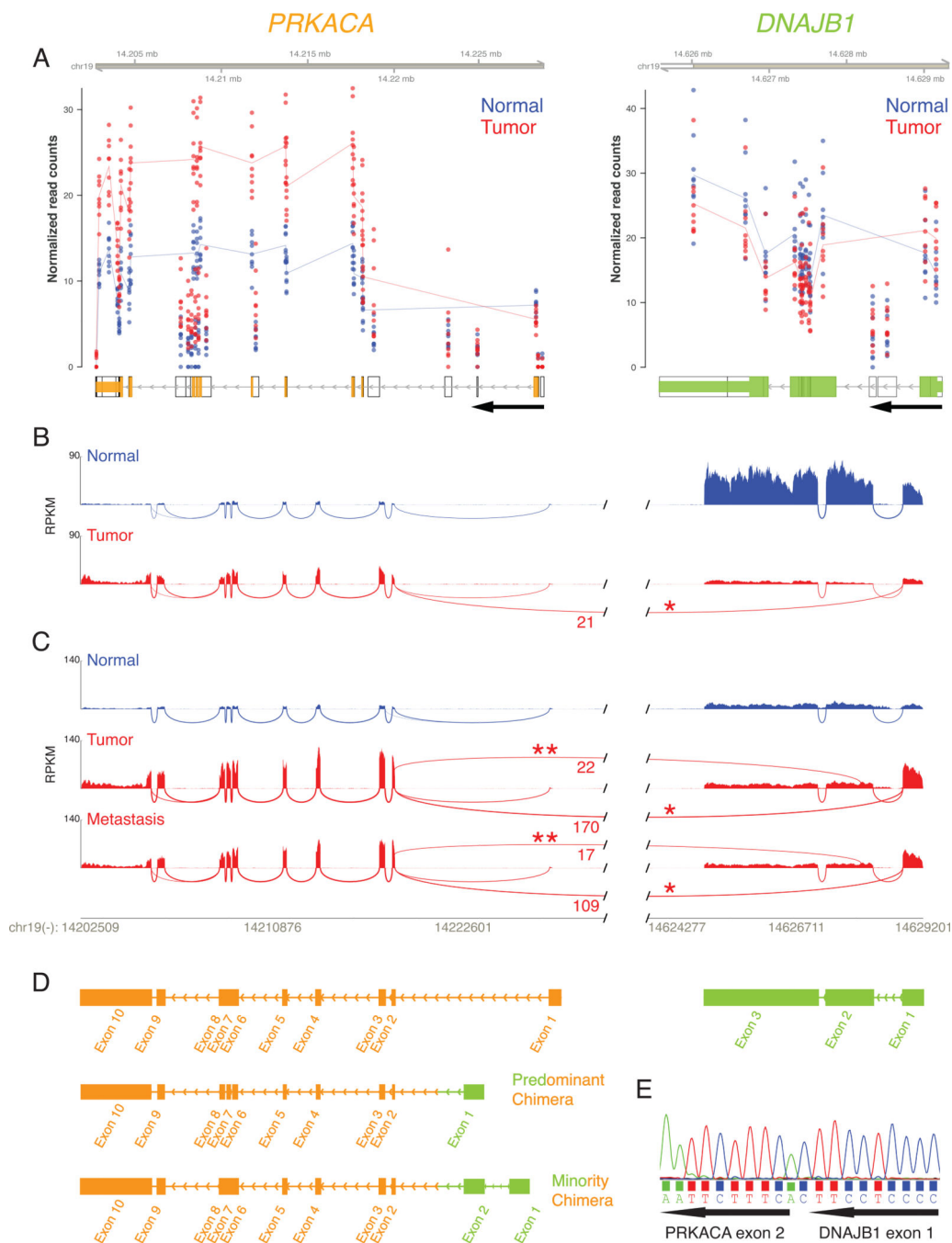


Fig. 1. RNA-seq read coverage from fibrolamellar hepatocellular carcinoma and adjacent healthy liver tissue
 (A-C) Plot of reads mapped to chromosome 19 in the region encoding on the negative strand the genes *PRKACA* (chr19:14,202,499 - 14,228,558) and *DNAJB1* (chr19:14,625,580 - 14,640,086) from the normal tissue (blue) and FL-HCC tissue (red). (A) Normalized RNA-Seq read counts from nine pairs of tumor and adjacent tissue demonstrate a consistent increase in tumor relative to normal in the reads of exon 2–10 of *PRKACA*, and a decrease in the reads of exon 1. Normalized read counts are plotted per exon part (non-overlapping

portions of exons in all isoforms in ENSEMBL annotation; indicated by empty grey boxes). Transcript structure (solid color boxes) indicates most likely dominant isoform as inferred by RNA-Seq read coverage. Lines indicate the average normalized read count per exon part (in dominant isoform) for normal and tumor samples. **(B)** Sashimi plot (39) of RNA-Seq read coverage at PRKACA and DNAJB1 loci for patient 9. Solid peaks depict reads per kilobase per million reads mapped (RPKM) within individual exons. Reads that bridge different exons are shown as arcs. In every tumor sample (9 out of 9) and in none of the normal tissue sample (0 out of 9), there are reads mapped from the end of exon 1 of DNAJB1 to the start of exon 2 of PRKACA. **(C)** There is an additional set of reads in patient 4 that map from the second exon of DNAJB1 to the start of the second exon of PRKACA. Indistinguishable results are observed in metastasis tissue from this same patient. **(D)** RNA-Seq read mapping predicts the production of four transcripts: a native DNAJB1 (green), a native isoform 1 PRKACA (orange), a predominant chimera with the first exon of DNAJB1 and exons 2–10 of PRKACA and, in a subset of patients, a minority transcript with the first exon and part of the second of DNAJB1 and exons 2–10 of PRKACA. **(E)**. Sanger Sequencing of RT-PCR products from FL-HCC samples confirmed a chimera transcript in 7 out of 7 patients joining the end of exon 1 of DNAJB1 and the start of exon 2 of PRKACA.

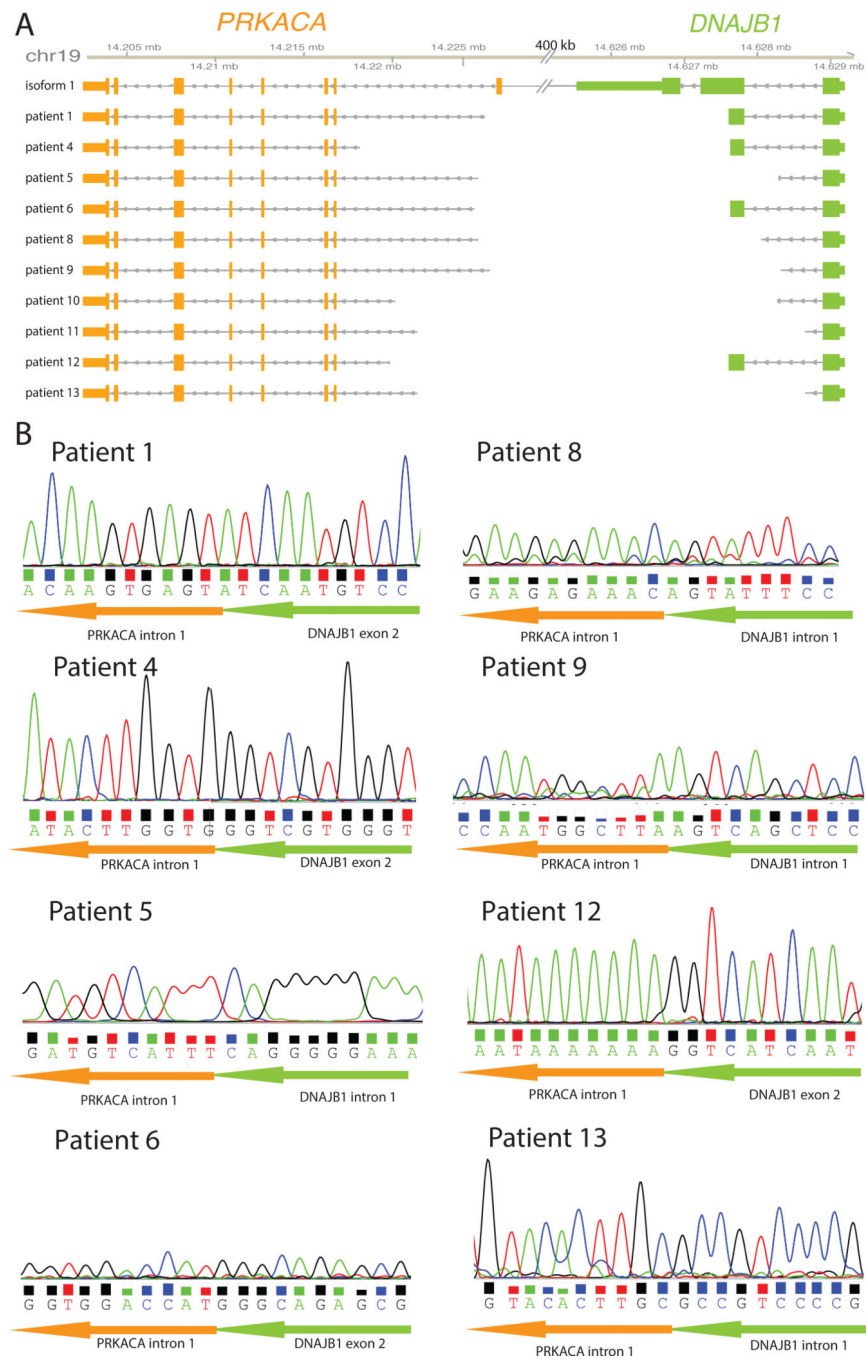


Fig. 2. DNA sequence analysis of fibrolamellar hepatocellular carcinoma DNA
 (A) Mapping of the size and location of the breaks in the DNA between the DNAJB1 and the PRKACA genes. (B). PCR followed by Sanger sequencing confirmed a deletion of ~400kD in each patient. Each deletion results in a fusion that starts either in intron 1 or exon 2 of DNAJB1 and ends in intron 1 of PRKACA. The break is in a different location in all patients. Note that the sequencing reads are shown off of the sense-strand. However, both DNAJB1 and PRKACA are coded off the negative strand.

2 of DNAJB1 and exon 2 of PRKACA (Patient 4, 14). **(B)** *Confirmation of Chimeric Protein*. Protein extracts of fibrolamellar carcinoma (T) and adjacent liver tissue (N) were immunoprecipitated with an antibody to the amino-terminus of DNAJB1 and run adjacent to total cell extract on SDS-PAGE. These samples were then subjected to immunoblot analysis using an antibody to the carboxyl-terminus of PRKACA **(C)** *PKA activity of WT PRKACA and Chimera are indistinguishable*. HEK-293T cells were transfected with an empty control plasmid, a plasmid encoding WT PRKACA, or a plasmid encoding the chimeric DNAJB1-PRKACA. Cell extracts were diluted and assayed for PKA activity. The activity of the WT PRKACA and the chimera PRKACA-DNAJB1 are significantly higher ($p < 0.001$, 2-way ANOVA) than background kinase activity. Samples were processed in triplicate \pm SEM. **(D and E)** *Immunofluorescence assay*. The presence and distribution of PRKACA protein was examined with an antibody against the carboxyl terminus in **(D)** adjacent normal and **(E)** FL-HCC liver tissue from patient 11 and imaged by confocal microscopy. The green areas correspond to PRKACA and the blue areas correspond to nuclei, which were stained with Hoechst. Similar results were seen in samples from additional patients (Supplemental Figure). Scale bar is 20 microns.